MINIATURE DRAG-FORCE ANEMOMETER

Lloyd N. Krause and Gustave C. Fralick

Lewis Research Center
Cleveland, Ohio 44135

1. Report No. NASA TM X-3507	2. Government Accession No.	3. Recipient's Catalog No.
4. Title and Subtitle MINIATURE DRAG-FORCE ANEMOMETER		5. Report Date June 1977
		6. Performing Organization Code
7. Author(s) Lloyd N. Krause and Gustave C. Fralick		8. Performing Organization Report No. E-9087
9. Performing Organization Name and Address Lewis Research Center National Aeronautics and Space Administration Cleveland, Ohio 44135		10. Work Unit No. 505-04
		11. Contract or Grant No.
12. Sponsoring Agency Name and Address National Aeronautics and Space Administration Washington, D.C. 20546		13. Type of Report and Period Covered Technical Memorandum
		14. Sponsoring Agency Code

15. Supplementary Notes

16. Abstract

A miniature drag-force anemometer is described which is capable of measuring dynamic velocity head and flow direction. The anemometer consists of a silicon cantilever beam 2.5 mm long, 1.5 mm wide, and 0.25 mm thick with an integrated diffused strain-gage bridge, located at the base of the beam, as the force-measuring element. The dynamics of the beam are like those of a second-order system with a natural frequency of about 42 kHz and a damping coefficient of 0.007. The anemometer can be used in both forward and reversed flow. Measured flow characteristics up to Mach 0.6 are presented along with application examples including turbulence measurements.

17. Key Words (Suggested by Author(s)) Anemometer; Flow direction; Velocity head; Turbulence measurement; Velocity measure- ment	18. Distribution Statement Unclassified - unlimited STAR Category 35		
19. Security Classif. (of this report) Unclassified	20. Security Classif. (of this page) Unclassified	21. No. of Pages 24	22. Price* A02

MINIATURE DRAG-FORCE ANEMOMETER

by Lloyd N. Krause and Gustave C. Fralick

Lewis Research Center

SUMMARY

A miniature drag-force anemometer is described which is capable of measuring dynamic velocity head and flow direction. The anemometer consists of a silicon cantilever beam 2.5 millimeters long, 1.5 millimeters wide, and 0.25 millimeter thick with an integrated diffused strain-gage bridge, located at the base of the beam, as the force-measuring element. The dynamics of the beam are like those of a second-order system with a natural frequency of about 42 kilohertz and a damping coefficient of 0.007. The anemometer can be used in both forward and reversed flow. Measured flow characteristics up to Mach 0.6 are presented along with application examples including turbulence measurements.

INTRODUCTION

This report describes a miniature drag-force anemometer, consisting of a cantilever beam with attached strain gages, which is capable of measuring dynamic velocity head and flow direction. The instrument was developed because the assortment of available instruments for determining dynamic flow quantities such as total pressure and velocity is limited and because measuring time-varying phenomena has become increasingly important in the developmental testing of airbreathing engines and their components.

The major types of dynamic flow diagnostic instrumentation in current use are miniature pressure transducers, mounted either in probes or duct walls, hot-wire and hot-film anemometers, and laser anemometers.

Laser anemometers are being used, to a limited extent, in applications where survey probes are impractical. Laser anemometers are used, for example, in transonic flows where probe blockage is excessive and in velocity surveys in the passages between rotating blades. High cost and the requirement of optical access have limited the application of laser anemometer systems.

Hot-wire and hot-film anemometers are also used to determine dynamic velocity. However, these instruments have a number of serious shortcomings. When used in compressible flows where density and temperature variations are not negligible, the anemometers require an elaborate calibration, and, even with a complete calibration, interpretation of results is difficult. Wire breakage and change in calibration due to flow contamination and/or corrosion are also problems. Each anemometer channel also requires an elaborate electronics package. The drag-force anemometer has the potential of overcoming some of the shortcomings of the hot-wire and hot-film anemometers. It is more rugged than a hot-wire anemometer, its calibration is simple and unaffected by flow contamination, and associated electronics are as simple as those of strain-gage pressure transducers.

The earliest reported use of the drag-force anemometer for dynamic flow measurement took place in compressor rotating-stall experiments (ref. 1), in which the natural frequency of the beam was 5 kilohertz. A different kind of anemometer was reported in reference 2. It consisted of an ogive-shaped body surrounding a piezoelectric element and was used to measure turbulence profiles in the wake of a circular cylinder in water. The instrument was capable of measurement at frequencies up to 1 kilohertz.

In the work described in this report an anemometer similar to that of reference 1 was used except that the natural frequency of the beam was much higher. The beam (which is commercially available) is silicon with an unclamped length of 2.5 millimeters and a thickness of 0.25 millimeter. A four-arm strain-gage bridge is bonded to the beam by solid-state diffusion techniques. The natural frequency of the beam in the first bending mode is about 42 kilohertz. This report describes the anemometer and its performance in subsonic flow. A brief discussion of initial applications is also included.

DESCRIPTION AND PRINCIPLE OF ANEMOMETER

Description of Anemometer

A photograph and a drawing of the drag-force anemometer used in this investigation are presented in figures 1 and 2, respectively. The silicon beam has an unsupported length of 2.5 millimeters with the outer 1.5 millimeters exposed to the flow. The width is also 1.5 millimeters, so the element exposed to the flow is a square plate which is 0.25 millimeter thick.

Water cooling passages in the region near the base of the beam allow the anemometer to be used at moderately elevated temperatures. The diffusion-bonded strain gages at the base of the unsupported length (fig. 3) are capable of operation at temperatures

up to 120° C. The water cooling also aids in minimizing stresses due to differences in thermal expansion between the silicon beam, the supporting metal, and the epoxy film which bonds the beam to the supporting metal.

The two longitudinal gages shown in figure 3 are the active gages which are either in tension or compression depending on to which side of the beam the flow is directed. Two transverse strain gages complete the Wheatstone bridge, and because the gages are near each other, the device is inherently temperature compensated. Because silicon is brittle like glass, the anemometer is fragile, and care is required in handling.

Principle of Operation

Velocity head measurement. - The drag force on the beam for flow normal to the beam surface is given by

$$D = C_D \frac{\rho U^2}{2} A \tag{1}$$

For constant beam area A, and constant drag coefficient C_D, the drag force D is proportional to the velocity head $\rho U^2/2$, where ρ and U are fluid density and velocity, respectively. Flow direction nomenclature is given in figure 4. (Symbols are defined in appendix A.) The variation of the flat-plate drag coefficient with several parameters is shown in figure 5 (from ref. 3). Figure 5(a) shows that the drag coefficient is insensitive to flow angle for angles within about 45° of normal to the beam surface. Figure 5(b) shows that effects due to variation in Reynolds number are negligible for Reynolds numbers greater than 10 000. As shown in figure 5(c), effects of variation in Mach number are small (within 5 percent) for Mach numbers less than 0.75. However, at transonic Mach numbers, variations in drag coefficient are not negligible and cause a nonlinear relation between drag force and velocity heat. (The Mach number sensitivity shown in fig. 5(c) is for a two-dimensional (or an infinitely high aspect ratio) plate, whereas the rest of the results of fig. 5 are for square plates.) Figure 5(d) shows that increasing the turbulence intensity from nearly zero to 5 percent results in a 5-percent increase in drag coefficient.

It should be noted that the drag-force anemometer can measure either forward or reversed velocity head. However, velocity can only be obtained from the velocity head when variations in density are negligible.

Flow direction measurement. - If the beam is oriented so that the flow is nearly parallel to the beam surface (fig. 4), the drag coefficient is proportional to flow angle, as shown in figure 5(a). (Strictly speaking, the term "drag coefficient" should be re-

3

placed with "lift coefficient" in this region. Hence, in this operating mode the drag-force anemometer would be more properly called the lift-force anemometer.) The output of the strain gage for this case is proportional to both flow angle and velocity head; so, when flow direction is measured, either two beams must be used or a single beam must be rotated to two positions (flow nearly normal to and flow nearly parallel to the beam surface). An alternative method of determining flow angle sensitivity is an in situ calibration which can be done if the anemometer is mounted in an actuator which can be rotated to known angular positions.

Sensitivity

For a rectangular beam of thickness t and width w, the strain at a point on the surface of the beam is

$$\text{strain} = \frac{6T}{Ewt^2} \tag{2}$$

where T is the bending moment at that point, and E is the Young's modulus of the beam material. The electrical output is proportional to the strain at the point where the bridge is located.

For the beam described in this report, the strain gages are centered at a distance l_1 (fig. 6) from the fixed end of the beam, and the part of the beam $L - l_2$ is exposed to the gas stream. If G is the electrical output per unit strain per volt of excitation, the signal per volt of excitation is

$$V = \frac{3C_D G}{Et^2} \frac{\rho U^2}{2} \left[(L - l_1)^2 - (l_2 - l_1)^2 \right] \tag{3}$$

The derivation of equation (3) is given in appendix B.

Natural Frequency and Damping Coefficient

The drag-force anemometer is a simple plane beam, supported at one end and free at the other. Its motion can be described by the wave equation for thin beams (ref. 4),

$$\frac{\partial^4 y}{\partial x^4} = -\frac{1}{c^2}\frac{\partial^2 y}{\partial \tau^2} \tag{4}$$

where y is the displacement of the beam from its equilibrium position, τ is time, x is the distance measured from the fixed end of the beam, and

$$c = \sqrt{\frac{EI'}{\rho'}} \tag{5}$$

in which E is Young's modulus, ρ' is the mass per unit length of the beam, and I' is the area moment of inertia of the beam cross section, $wt^3/12$.

Equation (4) may be solved by letting

$$y(x, \tau) = X(x)\Theta(\tau) \tag{6}$$

Substituting equation (6) into equation (4) gives the equation for Θ in the form

$$\frac{d^2\Theta}{d\tau^2} = -\omega^2\Theta \tag{7}$$

so that theoretically the frequency response of the beam is that of an undamped second-order system, with circular frequency ω. When the equation $X(x)$ is solved (for details see ref. 4), the natural frequency in the first bending mode is

$$f_n = \frac{\omega_n}{2\pi} = 0.1615\,\frac{t}{L^2}\sqrt{\frac{E}{\rho}} \tag{8}$$

where ρ is the density, the mass per unit volume.

In contrast to the situation for an ideal beam, there is a certain amount of damping present. The amount of damping is characterized by the parameter ζ, called the fraction of critical damping or the damping coefficient. It is equal to zero for an ideal (undamped) system and has the value 1 for a system which is critically damped.

The two parameters which characterize the beam, f_n and ζ, can be measured by using a spectrum analyzer. For a lightly damped second-order system, such as the drag-force anemometer considered in this report, the frequency spectrum of the strain-gage bridge signal is relatively flat at low frequencies, rises to a maximum at a frequency f_{max}, and finally drops off at higher frequencies. This is true as long as the

beam excitation can be characterized as a white noise source, a source whose spectrum is continuous and uniform as a function of frequency.

Let f_- be the frequency below f_{max} at which the amplitude is down 3 decibels from its value at f_{max} and f_+ be the frequency above f_{max} at which the amplitude is down 3 decibels from its maximum. The analysis given in appendix C shows that ζ and f_n are related to the location and width of the peak by

$$\zeta = \frac{f_+ - f_-}{2f_{max}} \tag{9}$$

and

$$f_n = \frac{f_{max}}{\sqrt{1 - 2\zeta^2}} \tag{10}$$

For highly underdamped beams, f_n and f_{max} are essentially equal.

CHARACTERISTICS OF ANEMOMETER

Basic Flow Characteristics

There are three basic flow characteristics of the drag-force anemometer: The first is the sensitivity of the anemometer to velocity head when the flow is normal to the beam surface. The second is the variation in the output due to any misalinement from the normal condition. The third is the angle sensitivity when the anemometer is used to measure flow direction.

Figure 7 illustrates the sensitivity to velocity head for values up to 0.25×10^5 newtons per square meter. The data were obtained in an ambient-temperature free jet. The maximum value for the velocity head shown corresponds to a Mach number of about 0.6. The sensitivity calculated from equation (3) and the manufacturer's nominal catalog value for the output of the strain-gage bridge on the beam (45 mV/V at 1000 microstrains (1 microstrain = 10^{-6} m/m)) was 15 percent greater than that obtained experimentally. This small disagreement is not unreasonable and could easily be due to deviation in the bridge sensitivity from the nominal catalog value. Also, the exposed portion of the beam is not of the exact same geometry as that for which the drag coefficient data of reference 3 were obtained. No attempt was made to calibrate the beam with known weights or loads because each anemometer should be calibrated in a flowing

stream. Such a calibration would include effects of local flow acceleration in the region of the beam tip. For reversed flow, the sensitivity is the same magnitude as that of figure 7 but with a negative sign.

The anemometer is quite insensitive to angular misalinement about an axis passing through the beam support for nearly normal flow incidence, as shown in figure 8 (β variation). The output voltage is essentially constant over a range of β of $\pm 20^O$ from normal. However, variation in output voltage with variation in α is not negligible, and an approximate value for α must be known to ensure adequate accuracy in velocity head measurement (see fig. 4 for definition of α and β).

As indicated by figure 9, when the anemometer is used to measure flow direction, it is highly desirable to orient the beam so that α is the angle of measurement. For α measurement the longitudinal strain gages (fig. 3) are either in compression or tension, and the transverse gages are not under strain, so that a workable sensitivity curve is obtained. However, if the beam is oriented so that β is the angle of measurement, a more highly nonlinear and asymmetrical sensitivity curve is obtained. The asymmetry is probably due to the contribution of the transverse gages as the beam is subjected to a torque during β variation.

The slope of the α sensitivity curve of figure 9 is approximately the same as a calculated slope based on the curve of figure 5(a). With the beam and tip geometry used, the stall region (fig. 5(a)) on the α curve does not occur until the flow angle is greater than 50°. The curves of figure 9 are for a velocity head of 0.1×10^5 newtons per square meter. The output voltage at a given flow angle is proportional to the velocity head.

The small output at zero flow angle is due to the fluid dynamic force on the edge of the beam, which causes a slight strain in the strain gages at the base of the beam (the edge thickness is 1/6 of the width).

Frequency Response

The drag-force anemometer response is that of a highly underdamped second-order system with a high natural frequency. The natural frequency is 41.8 kilohertz, and the damping coefficient is 0.007. These were measured with a spectrum analyzer (fig. 10), as explained in the section Natural Frequency and Damping Coefficient. A small jet was the white noise excitation source for the beam motion. The natural frequency of the beam calculated from equation (8) by using a density of 2.42×10^3 kilograms per cubic meter and a Young's modulus of 1.6×10^{11} newtons per square meter is 52 kilohertz, which is 20 percent higher than the measured value. Changing the effective length of the beam by only 0.25 millimeter would account for the difference between measured and calculated values.

The high natural frequency makes the drag-force anemometer useful up to approximately 10 kilohertz. The fact that the silicon beam with diffused strain gages is very nearly an ideal second-order system suggests that it can be electronically compensated (ref. 5) and that the frequency response can be extended to 100 kilohertz or beyond.

Zero Drift and Sensitivity Stability

As mentioned previously, the beam is inherently temperature compensated because the four strain gages are located close to each other. However, the beam can be subjected to thermal stresses in the region of the strain gages because of the differences in thermal expansion among the beam, the metal support, and the epoxy which bonds the beam to the support. For the anemometer described in this report, the silicon beam with an expansion coefficient of 2.5×10^{-6} per ^{O}C was bonded to stainless steel (expansion coefficient of $18 \times 10^{-6}/^OC$) with an epoxy whose coefficient was about 90×10^{-6} per ^{O}C. The normal zero drift and the drift in zero associated with the thermal expansion problem can be minimized by setting the zero on the anemometer before each run and checking it immediately following the run. Preferably, zero settings should be made with the beam at fluid temperature. When the results shown in figure 7 were generated, in a nearly ambient-temperature air jet, zero drifts were typically less than 0.02 millivolt.

The drift associated with thermal expansion can probably be reduced by using a beam support material such as Invar, with thermal expansion nearly matching that of silicon. Also, silicon beams are available that are inorganically bonded to a glass pedestal, which decreases the effect of the epoxy mounting joint because the joint is farther from the strain gages.

If only the ac portion of the dynamic velocity head is of interest in a particular application, zero drift is of no concern. However, the stability of the sensitivity is of concern. During testing of the anemometer, the sensitivity remained constant except for the fan jet engine application described in the section APPLICATIONS. During the engine run, the silicon beam was exposed to a gas temperature in excess of 150° C, which was beyond the recommended operating temperature of 120° C. The overtemperature exposure resulted in a permanent decrease in sensitivity of about 30 percent.

APPLICATIONS

Because of the preliminary nature of the work described in this report, only two applications have been tested thus far. In the first, the drag-force anemometer was used to measure the intensity of turbulence of a room-temperature air jet. The

8

relation between anemometer output and turbulence is as follows.

If the instantaneous velocity U_{inst} contains only frequency components small compared with the natural frequency of the beam, the relation between the output voltage and the velocity of a constant-density gas stream is

$$V_{inst} = KU_{inst}^2 \qquad (11)$$

where

$$V_{inst} = V + v$$

$$U_{inst} = U + u \qquad (12)$$

so that

$$V + v = K(U + u)^2$$

$$= K(U^2 + 2uU + u^2) \qquad (13)$$

The mean electrical output V is related to the mean velocity U by

$$V = KU^2 \qquad (14)$$

so that dropping the u^2 term results in

$$v = 2uKU \qquad (15)$$

If equation (15) is divided by equation (14), the result is

$$\frac{u}{U} = \frac{v}{2V} \qquad (16)$$

Squaring equation (16), taking the mean, and then taking the square root give

$$\frac{\sqrt{\overline{u^2}}}{U} = \frac{\sqrt{\overline{v^2}}}{2V} \qquad (17)$$

The drag-force anemometer was used to measure the turbulence intensity in the free jet described in reference 6. The turbulence intensity was measured at two locations with both the drag-force anemometer and a hot-wire anemometer. The bandwidth was 10 kilohertz for both measurements. On the jet centerline 0.57 jet diameter downstream from the start of the jet, both the hot-wire and drag-force anemometers measured an intensity of 1.8 percent. At 2.29 diameters downstream from the start of the jet and 0.2 diameter from the jet centerline, the hot-wire anemometer measured a 4.3-percent intensity and the drag-force anemometer measured a 3.8-percent intensity. These hot-wire measurements are also in agreement with those taken previously (ref. 6) to within the accuracy of the hot-wire anemometer.

In the second application, a drag-force anemometer was inserted in a turbofan engine in the annulus downstream of the first fan rotor. The anemometer was used as a diagnostic instrument to aid in determining possible changes between flutter and non-flutter flow conditions of the first fan rotor. Typical results are shown in figure 11. Figure 11(a) shows the variation in dynamic flow angle for several blade passages. The blade passing frequency is about 5 kilohertz. Figure 11(a) is the profile obtained by averaging 64 time traces of the same blade passages. The ordinate in figure 11(b) is proportional to the power spectral density of the anemometer output signal. The largest peak represents the blade passing frequency. There are frequencies present in figure 11(b) which are not multiples of the engine speed, and these can be correlated to flutter frequencies.

CONCLUSIONS

A drag-force anemometer has been developed which is capable of dynamic flow measurement. The anemometer consists of a silicon beam 2.5 millimeters long and 0.25 millimeter thick with an integral diffused strain-gage bridge as the force-measuring element. The following conclusions were drawn from tests of its performance in subsonic flow:

1. When the anemometer is oriented so that flow is nearly perpendicular to the beam surface, the output of the strain-gage bridge is proportional to the velocity head. Over the range of Mach numbers from 0 to 0.6, the output is linear with velocity head to within the accuracy of measurement.

2. The anemometer can be used in both forward and reversed flow.

3. The anemometer is capable of measuring flow direction when the beam is oriented so that flow is nearly parallel to the beam surface. However, for nearly parallel flow the output is proportional to both flow angle and velocity head, so that two measurements are required if the anemometer is used for flow angle determination. The beam is capable of measuring flow angles in excess of $\pm 40^{\circ}$.

10

4. Under dynamic flow conditions, the anemometer has a frequency response like that of a highly underdamped second-order system with a natural frequency of 41.8 kilohertz and a damping coefficient of 0.007.

5. The anemometer can be used to measure turbulence intensity. The intensity, for incompressible flow, in the direction normal to the beam surface is simply the rms value of the bridge output divided by twice the mean value.

6. The anemometer performed satisfactorily in two applications. In the first, the anemometer was used to measure turbulence intensity in a free jet, and the results agreed with those measured with a hot-wire anemometer. In the second, the drag-force anemometer was used as a diagnostic instrument during fan flutter tests of a fan jet engine. Frequencies were detected in the rotor blade wakes which were not multiples of the engine speed as well as frequencies which were multiples of the engine speed.

Lewis Research Center,
National Aeronautics and Space Administration,
Cleveland, Ohio, March 31, 1977,
505-04.

APPENDIX A

SYMBOLS

A area of beam, m^2

C_B proportionality constant in eq. (C1), $(mV)(m^2)/N$

C_D drag coefficient

c parameter in beam equation, eq. (5), m^2/sec

D drag force on beam, N

E Young's modulus, N/m^2

F amplitude of white noise driving force, N/m^2

f_{max} frequency at maximum amplitude, Hz

f_n first bending natural frequency, Hz

f_+, f_- frequencies 3 dB above and below f_{max}, Hz

G gage factor, $(mV/V)/microstrain$

I' area moment of inertia of beam, m^4

K proportionality constant in eq. (11), $(mV)(sec^2)/m^2$

L length of beam, m

l_1 distance of strain gage from fixed end of beam, m

l_2 length of beam not exposed to gas stream, m

M Mach number

Re Reynolds number

S shearing force at a point on beam, N

T bending moment at a point on beam, $(N)(m)$

t thickness of beam, m

U mean velocity of gas stream, m/sec

U_{inst} instantaneous velocity of gas stream, m/sec

u fluctuation in gas stream velocity, m/sec

V mean electrical output of beam, mV

V_{inst} instantaneous electrical output of beam, mV

v fluctuation in electrical output of beam, mV

w   width of beam, m

X   x-dependent factor of y

x   coordinate distance along length of beam, m

Y   vertical force per unit length, N/m

y   displacement of beam from equilibrium position, m

α, β angles describing orientation of beam, deg

ζ damping coefficient

Θ time dependent factor of y

ρ density, kg/m^3

ρ' density per unit length, kg/m

τ time, sec

ω circular frequency, rad/sec

ω_n natural circular frequency, rad/sec

APPENDIX B

DERIVATION OF EQUATION (3)

For a rectangular beam of thickness t and width w, the strain at a point on the surface of the beam is

$$\text{strain} = \frac{6T}{Ewt^2} \qquad (2)$$

where T is the bending moment at that point, and E is the Young's modulus of the beam material. The electrical output is proportional to the strain at the point where the bridge is located.

For the beam described in this report, the strain gages are centered at a distance l_1 (fig. 6) from the fixed end of the beam, and the part of the beam $(L - l_2)$ is exposed to the gas stream.

In order to calculate the output, it is necessary to calculate the bending moment at l_1, in order to use equation (2). At each point on the beam, the following equations are true (ref. 7):

$$\frac{dS}{dx} = Y \qquad (B1)$$

$$\frac{dT}{dx} = -S \qquad (B2)$$

where

S   shear force, positive upward

x   distance along beam from fixed end

Y   external vertical force per unit length

T   bending moment, positive counterclockwise

The weight of the beam is neglected in these calculations, so that in the region $0 \leq x \leq l_2$, Y = 0. Then, from equation (B1), S is constant in this region. This constant can be evaluated by noting that at x = 0 the wall must exert a shear force equal to the force exerted by the gas stream, which is $C_D w(\rho U^2/2)(L - l_2)$. Thus,

$$S = C_D w \frac{\rho U^2}{2} (L - l_2) \tag{B3}$$

From equations (B2) and (B3),

$$T = -C_D w \frac{\rho U^2}{2} (L - l_2)x + C \tag{B4}$$

The unknown constant in equation (B4) may be found by evaluating the bending moment at $x = 0$, which is equal to the bending moment due to the gas stream. The constant is then

$$C = \int_{l_2}^{L} C_D \frac{\rho U^2}{2} wx \, dx = \frac{C_D w}{2} \frac{\rho U^2}{2} \left(L^2 - l_2^2 \right) \tag{B5}$$

When equations (B4) and (B5) are combined, the bending moment T at $x = l_1$ is

$$T = -C_D w \frac{\rho U^2}{2} (L - l_2)l_1 + \frac{C_D w}{2} \frac{\rho U^2}{2} \left(L^2 - l_2^2 \right)$$

which simplifies to

$$T = \frac{C_D w}{2} \frac{\rho U^2}{2} \left[(L - l_1)^2 - (l_2 - l_1)^2 \right] \tag{B6}$$

If G is the electrical output per unit strain per volt of excitation from the strain-gage bridge, the signal per volt of excitation is, from equations (2) and (B6),

$$V = \frac{3C_D G}{Et^2} \frac{\rho U^2}{2} \left[(L - l_1)^2 - (l_2 - l_1)^2 \right] \tag{3}$$

PROCEDURE FOR USING SPECTRUM ANALYZER TO FIND NATURAL FREQUENCY

AND DAMPING COEFFICIENT OF SECOND-ORDER SYSTEM

DRIVEN BY WHITE NOISE SOURCE

If a second-order system is driven by a sinusoidal forcing function $F \cos \omega\tau$, the amplitude of the output is

$$B = \frac{C_B F}{\sqrt{\left(1 - \frac{\omega^2}{\omega_n^2}\right)^2 + 4\zeta^2 \frac{\omega^2}{\omega_n^2}}} = \frac{C_B F}{\sqrt{\left(1 - \frac{f^2}{f_n^2}\right)^2 + 4\zeta^2 \frac{f^2}{f_n^2}}} \qquad (C1)$$

For a white noise source, F is a constant, independent of frequency, and C_B is a proportionality constant.

Let f_{max} be the frequency at which the amplitude is maximum. This quantity, which is obtained directly from the spectrum analyzer, is found by differentiating B and setting $dB/df = 0$. Then,

$$\frac{dB}{df} = \frac{-2 \frac{f^2}{f_n^2}\left[\frac{f^2}{f_n^2} - (1 - 2\zeta^2)\right]}{\left[\left(1 - \frac{f^2}{f_n^2}\right)^2 + 4\zeta^2 \frac{f^2}{f_n^2}\right]^{3/2}} C_B F$$

which is zero at $f^2 = f_n^2(1 - 2\zeta^2)$, or

$$f_n = \frac{f_{max}}{\sqrt{1 - 2\zeta^2}} \qquad (10)$$

If only the natural frequency is desired, it is generally safe to just read f_{max} from the spectrum analyzer and use $f_n \simeq f_{max}$. Even for $\zeta = 0.1$, which is a higher

value than is likely to be encountered, equation (10) shows that the error is only about 1 percent.

When $f = f_{max}$ is inserted in equation (C1), the maximum amplitude is

$$B_{max} = \frac{C_B F}{2\zeta \sqrt{1 - \zeta^2}} \qquad (C2)$$

If F were known, equation (C2) could be used to find ζ, and equation (10) could be used to find f_n. In general, however, F is not known. Instead, use is made of the fact that ζ is related to the width of the peak at $f = f_{max}$.

Let f_- be the frequency below f_{max} at which the amplitude is $B_{max}/\sqrt{2}$ and f_+ be the frequency above f_{max} at which the amplitude is $B_{max}/\sqrt{2}$. On a spectrum analyzer with a log scale, these are the frequencies at which the amplitude is down 3 dB from the maximum value.

In order to find f_- and f_+, it is necessary to solve the equation

$$\frac{C_B F}{2\sqrt{2} \, \zeta \sqrt{1 - \zeta^2}} = \frac{C_B F}{\sqrt{\left(1 - \frac{f^2}{f_n^2}\right)^2 + 4\zeta^2 \frac{f^2}{f_n^2}}}$$

With $m = f/f_n$, this equation becomes

$$(m^2 - 1)^2 + 4\zeta^2 m^2 = 8\zeta(1 - \zeta^2) \qquad (C3)$$

Equation (C3) may be rewritten as

$$(m^2 - 1)^2 + 4\zeta^2(m^2 - 1 + 1) = 8\zeta^2(1 - \zeta^2)$$

so that with the substitution $n = m^2 - 1$, equation (C3) becomes

$$n^2 + 4\zeta^2 n - 4\zeta^2(1 - 2\zeta^2) = 0 \qquad (C4)$$

The roots of equation (C4) are

$$n = -2\zeta^2 \pm 2\zeta \sqrt{1 - \zeta^2}$$

or

$$m^2 = 1 - 2\zeta^2 \pm 2\zeta \sqrt{1 - \zeta^2}$$

$$\frac{f^2}{f_n^2} = (1 - 2\zeta^2)\left(1 \pm \frac{2\zeta \sqrt{1 - \zeta^2}}{1 - 2\zeta^2}\right)$$

Together with equation (10) they give

$$f_\pm = f_{max}\left(1 \pm \frac{2\zeta \sqrt{1 - \zeta^2}}{1 - 2\zeta^2}\right)^{1/2} \tag{C5}$$

If it assumed that the damping coefficient is very small, the quantity involving ζ in equation (C5) may be expanded in a Taylor series about $\zeta = 0$, keeping only the terms first order in ζ. When this is done, the result is

$$f_+ \simeq f_{max}(1 + \zeta)$$

$$f_- \simeq f_{max}(1 - \zeta)$$

Solving for ζ gives

$$\zeta \simeq \frac{f_+ - f_-}{2f_{max}} \tag{9}$$

Equations (10) and (9) give the damping coefficient and natural frequency in terms of quantities which can be directly measured on a spectrum analyzer.

18

REFERENCES

1. Beknev, V. S.; Zemlyanskiy, A. V.; and Tumashev, R. Z.: Experimental Study of Rotating Stall in High-Pressure Stages of an Axial-Flow Compressor. NASA TTF-15,115, 1973. (Mashinostr., no. 8, 1970, pp. 116-122.)

2. Siddon, Thomas E.: A New Type Turbulence Gauge for use in Liquids. Flow - Its Measurement and Control in Science and Industry. Vol. 1, pt. 1, Rodger B. Dowdell, ed., Instrum. Soc. Am., 1974, pp. 435-439.

3. Hoerner, Sighard F.: Fluid-Dynamic Drag; Practical Information on Aerodynamic Drag and Hydrodynamic Resistance. Midland, 1965.

4. Sommerfeld, Arnold: Partial Differential Equations in Physics. Academic Press., Inc., 1949, p. 303.

5. Schweppe, J. L.; et al.: Methods for the Dynamic Calibration of Pressure Transducers. NBS-Monograph-67, Nat. Bur. Stand., 1963.

6. Lawrence, James C.: Intensity, Scale, and Spectra of Turbulence in Mixing Region of Free Subsonic Jet. NACA Rep. 1292, 1957.

7. Synge, John L.; and Griffith, Byron A.: Principles of Mechanics. 3rd ed., McGraw-Hill, 1959.
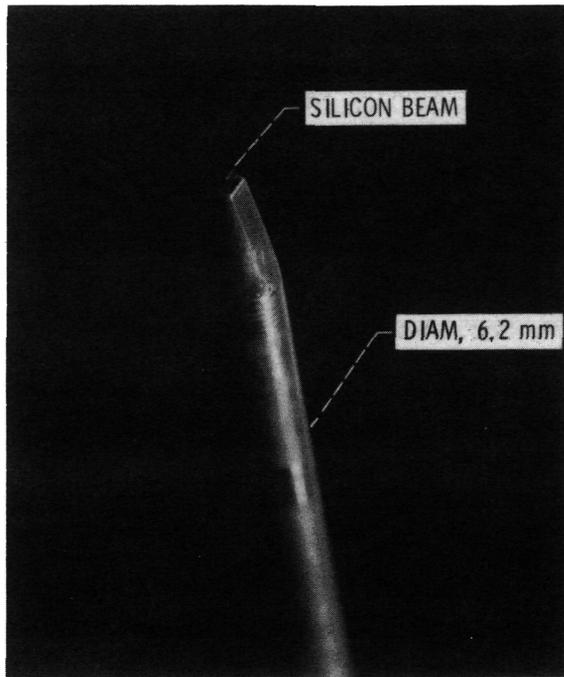
Figure 1. - Drag-force anemometer.

1.5 mm

A A

Silicon beam

Water cooling
passage

Strain-gage
lead wires

A-A

6.2-mm-diam tube
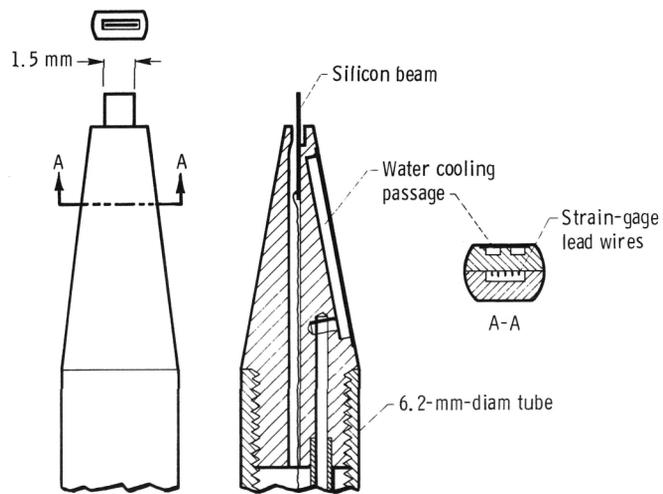
Figure 2. - Detail of drag-force anemometer.
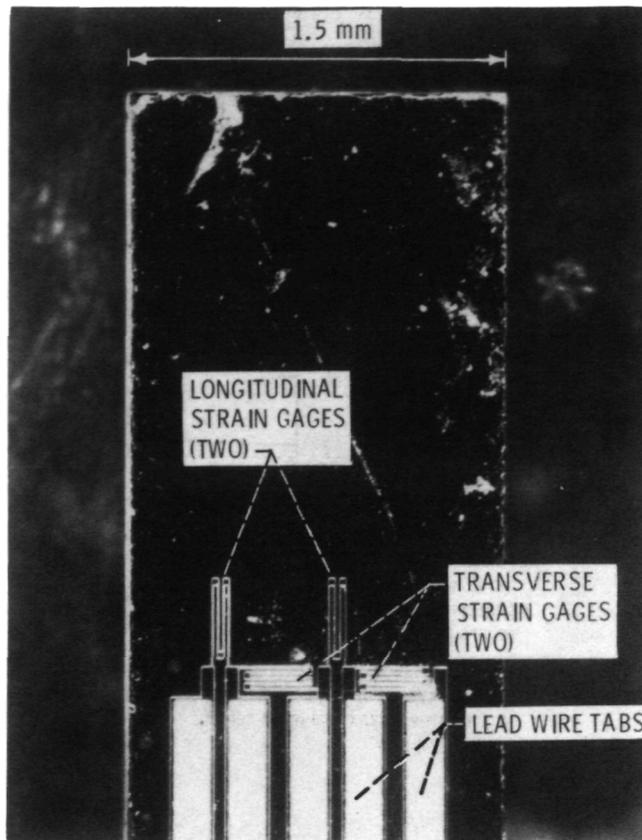
Figure 3. - Silicon beam.
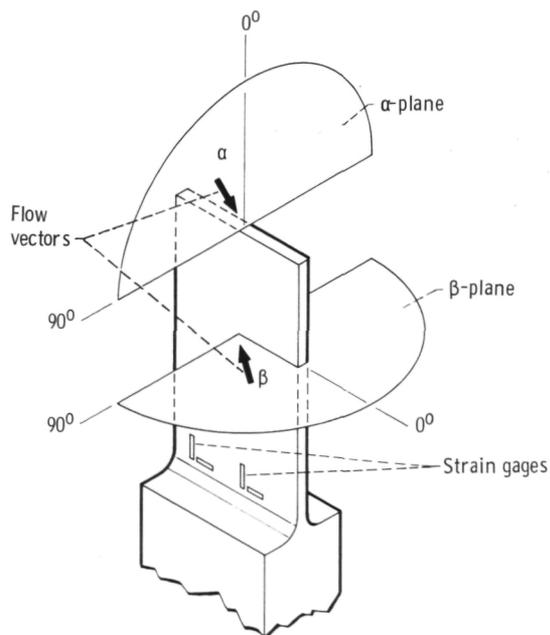
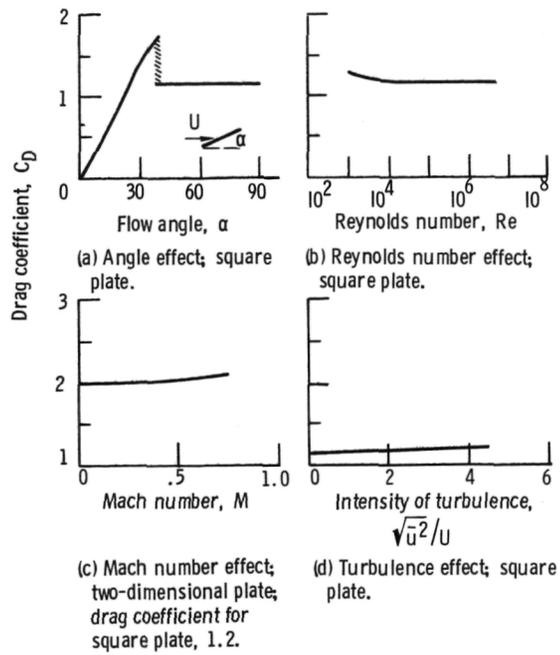Figure 4. - Flow-direction nomenclature. For flow normal to beam, α and $\beta = 90^0$.

21

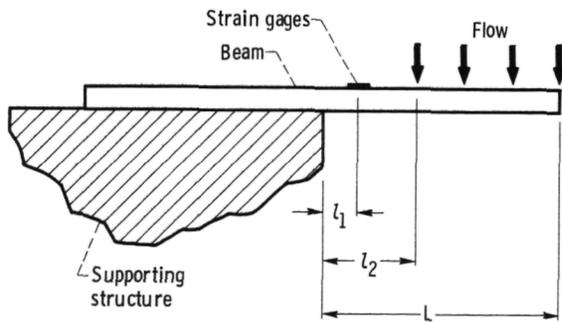Figure 5. - Variation of flat-plate drag coefficient with various flow parameters (from ref. 3).

(a) Angle effect; square plate.

(b) Reynolds number effect; square plate.

(c) Mach number effect; two-dimensional plate; drag coefficient for square plate, 1.2.

(d) Turbulence effect; square plate.

Figure 6. - Beam-dimension nomenclature.
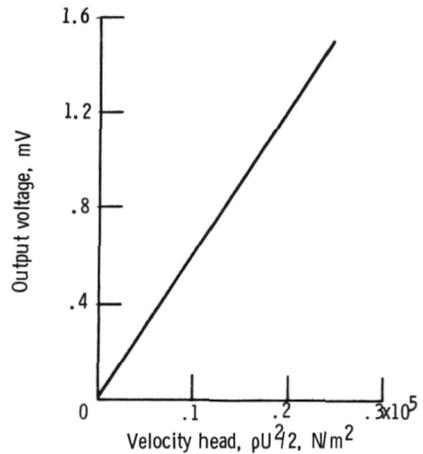
Figure 7. - Drag-force anemometer sensitivity for flow normal to beam surface. Bridge input voltage, 1 volt.
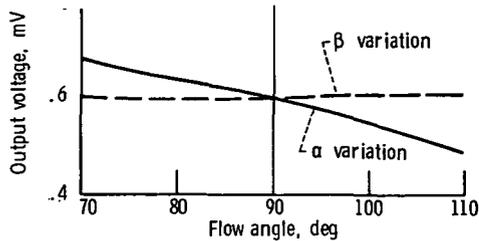
Figure 8. – Sensitivity of drag-force anemometer to flow angle variations from normal to beam surface. Velocity head, 0.1×10^5 newtons per square meter; bridge input voltage, 1 volt.
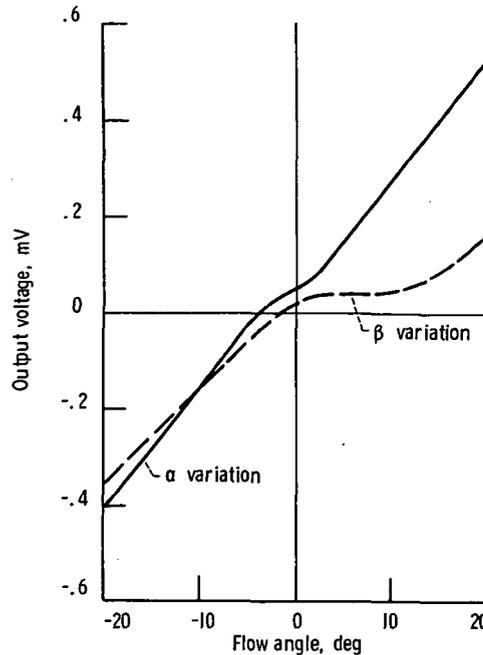
Figure 9. – Sensitivity of drag-force anemometer to flow angle variations near 0^0. Velocity head, 0.1×10^5 newtons per square meter; bridge input voltage, 1 volt.
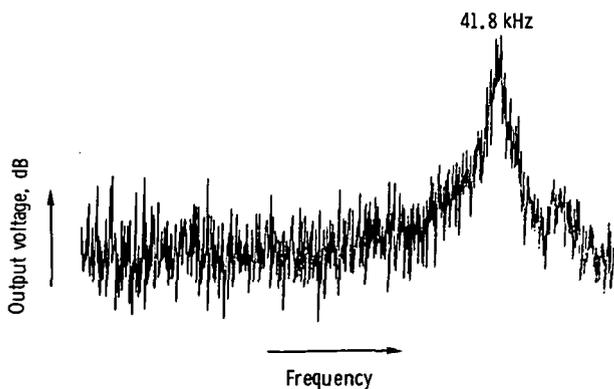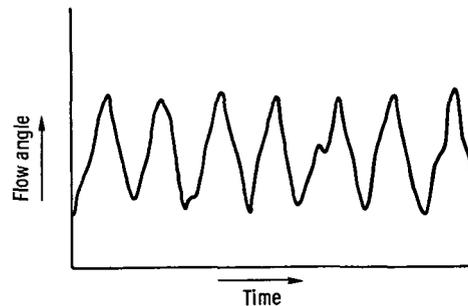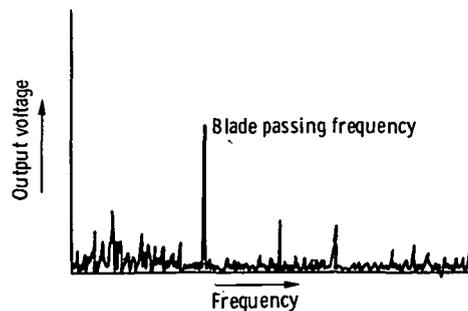

Figure 10. – Frequency spectrum of drag-force anemometer.

(a) Dynamic flow angle.

(b) Frequency spectrum

Figure 11. – Drag-force anemometer measurements taken downstream of fan rotor in turbofan engine.

"The aeronautical and space activities of the United States shall be conducted so as to contribute . . . to the expansion of human knowledge of phenomena in the atmosphere and space. The Administration shall provide for the widest practicable and appropriate dissemination of information concerning its activities and the results thereof."
—NATIONAL AERONAUTICS AND SPACE ACT OF 1958

NASA SCIENTIFIC AND TECHNICAL PUBLICATIONS

TECHNICAL REPORTS: Scientific and technical information considered important, complete, and a lasting contribution to existing knowledge.

TECHNICAL NOTES: Information less broad in scope but nevertheless of importance as a contribution to existing knowledge.

TECHNICAL MEMORANDUMS: Information receiving limited distribution because of preliminary data, security classification, or other reasons. Also includes conference proceedings with either limited or unlimited distribution.

CONTRACTOR REPORTS: Scientific and technical information generated under a NASA contract or grant and considered an important contribution to existing knowledge.

TECHNICAL TRANSLATIONS: Information published in a foreign language considered to merit NASA distribution in English.

SPECIAL PUBLICATIONS: Information derived from or of value to NASA activities. Publications include final reports of major projects, monographs, data compilations, handbooks, sourcebooks, and special bibliographies.

TECHNOLOGY UTILIZATION PUBLICATIONS: Information on technology used by NASA that may be of particular interest in commercial and other non-aerospace applications. Publications include Tech Briefs, Technology Utilization Reports and Technology Surveys.

Details on the availability of these publications may be obtained from:

SCIENTIFIC AND TECHNICAL INFORMATION OFFICE

NATIONAL AERONAUTICS AND SPACE ADMINISTRATION
Washington, D.C. 20546